Fermi National Accelerator Laboratory

FERMILAB-PUB-91/70-T

BNL-45990

March 1991

QCD Correction to the $pp \to WH$ and ZH Total Cross Sections

T. Han

Fermi National Accelerator Laboratory

P.O. Box 500, Batavia, IL 60510

and

S. Willenbrock

Brookhaven National Laboratory

Upton, NY 11973

Abstract

We calculate the QCD correction to the total cross section for the production of a Higgs boson in association with a W or Z boson at the LHC/SSC. The QCD-corrected cross section is insensitive to the choice of factorization and renormalization scales. Setting these scales to the invariant mass of the VH final state, the QCD correction increases the lowest-order cross section by about 17/15 percent in the DIS factorization scheme, and 12/10 percent in the $\overline{\rm MS}$ scheme, at the LHC/SSC.

Operated by Universities Research Association Inc. under contract with the United States Department of Energy

The search for the standard-model Higgs boson is one of the most important experimental challenges for present and future colliders. LEP I has set a lower bound of 48 GeV on the Higgs-boson mass; [1] it will ultimately extend the search to 55-60 GeV. LEP II will be able to explore up to a Higgs-boson mass of approximately 80 GeV. If no Higgs boson is found, we must await the completion of the LHC/SSC in order to explore larger Higgs-boson masses.

If $m_H > 2M_Z$, it will be straightforward to detect a Higgs boson at the LHC/SSC decaying via $H \to ZZ \to 4$ leptons, up to a mass of at least 800 GeV. Less straightforward is the intermediate mass region, 80 GeV $\lesssim m_H < 2M_Z$. The decay mode $H \to ZZ^* \to 4$ leptons [2,3] should allow detection of a Higgs boson of mass 140 GeV $\lesssim m_H < 2M_Z$. Below 140 GeV, the decay $H \to \gamma\gamma$ [3,4] may yield an observable signal if excellent photon energy resolution and photon/jet discrimination are achieved.

Recently, much progress has been made in the detection of a Higgs boson of mass 80 GeV $\lesssim m_H \lesssim$ 140 GeV. The production of a Higgs boson in association with a W boson, [5] followed by $H \to \gamma\gamma$ and $W \to \ell\bar{\nu}$, provides a nearly background-free signal even with modest photon energy resolution and photon/jet discrimination.[6,7] The number of events is rather small, however. Even more promising is the production of a Higgs boson in association with a top-antitop pair, [8] followed by $H \to \gamma\gamma$ and $t \to b\bar{\ell}\nu$ or $\bar{t} \to \bar{b}\ell\bar{\nu}$. [9,10] The rate for this process is roughly twice that of the WH process at the LHC, and roughly five times that of the WH process at the SSC. In both processes the signal is two photons and an isolated, high transverse-momentum charged lepton.

The WH process depends on the HW^+W^- coupling, while the $t\bar{t}H$ process depends on the Yukawa coupling of the Higgs-boson to the top quark. Measuring these processes separately will determine the ratio of the HW^+W^- and $Ht\bar{t}$ couplings,

making no assumption about the $H \to \gamma\gamma$ branching ratio.[10] It may also be possible to detect other decay modes of the Higgs boson.

Due to the modest number of signal events, it is important to calculate the production cross sections as accurately as possible. The calculation of any cross section at the LHC/SSC is plagued by uncertainty in the choice of the factorization scale in the parton distribution functions, as well as the uncertainty in the distribution functions themselves. The former uncertainty can be reduced by calculating at next-to-leading order in QCD; the latter will be reduced when data from HERA, and the LHC/SSC themselves, become available.

In this paper we calculate the QCD correction to the total cross section for the production of a Higgs boson in association with a W or Z boson at the LHC/SSC. The QCD-corrected cross section is insensitive to the choice of the factorization scale, and thus provides a more reliable estimate of the total cross section than the lowest-order calculation. The dominant remaining uncertainty in the cross section is the choice of parton distribution functions. The analogous calculation for the production of a Higgs boson in association with a top-antitop pair is also of interest, but is technically much more difficult.

The production of a Higgs boson in association with a vector boson, V, proceeds at tree level via the subprocess $q\bar{q} \to V^* \to VH$. The QCD correction to this process, for a given mass of the virtual boson, is exactly the same as the QCD correction to the Drell-Yan process, as pointed out in Refs. [6,11]. To obtain the total cross section, we must incorporate the decay of the virtual boson to VH and integrate over its mass.

Consider the modulus squared of the amplitude for a virtual vector boson of momentum q to decay to VH. Summing over the polarizations of the final vector

boson and integrating over the two-particle phase space, we obtain

$$I^{\mu\nu}(q^2) = \frac{\sqrt{2}G_F M_V^4}{\pi}\frac{|\mathbf{p}|}{\sqrt{q^2}}\Big[- g^{\mu\nu}\left(1+\frac{1}{3}\frac{|\mathbf{p}|^2}{M_V^2}\right) + \frac{q^\mu q^\nu}{q^2}\left(1+\frac{4}{3}\frac{|\mathbf{p}|^2}{M_V^2}\right)\Big] \qquad (1)$$

where $|\mathbf{p}|$ is the common momentum of the final-state particles in the V^* rest frame,

$$|\mathbf{p}| = \frac{1}{2\sqrt{q^2}}\lambda^{\frac{1}{2}}(q^2, M_V^2, m_H^2), \qquad (2)$$

with

$$\lambda(a,b,c) \equiv a^2 + b^2 + c^2 - 2ab - 2ac - 2bc. \qquad (3)$$

The indices on the function I refer to the polarization of the virtual boson.[1]

The current to which the vector boson couples is conserved to all orders in QCD (for massless quarks). The $q^\mu q^\nu$ term in $I^{\mu\nu}$ therefore does not contribute to the cross section. The $-g^{\mu\nu}$ term replaces the sum on the polarizations of the virtual vector boson. Therefore

$$\frac{d\sigma}{dq^2}(pp \to VH + X) = \sigma(pp \to V^* + X)\frac{1}{2\pi(q^2 - M_V^2)^2}\frac{\sqrt{2}G_F M_V^4}{\pi}\frac{|\mathbf{p}|}{\sqrt{q^2}}\left(1+\frac{1}{3}\frac{|\mathbf{p}|^2}{M_V^2}\right) \qquad (4)$$

to all orders in QCD. The total cross section is obtained by integrating over q^2.

The $\mathcal{O}(\alpha_S)$ correction to the total Drell-Yan cross section has been known for over ten years [12,13]. Rather than reproducing the expressions here, we simply remind the reader that the cross section depends on the factorization scale μ both in the parton distribution functions and explicitly in the matrix element at $\mathcal{O}(\alpha_S)$. Since the explicit dependence is proportional to $\ln(\mu^2/q^2)$, the choice $\mu = \sqrt{q^2} \equiv M_{VH}$ is natural to avoid large logarithms. The cross section also depends weakly on the renormalization

[1] $I^{\mu\nu}$ may also be regarded as twice the imaginary part of the vector-boson self energy due to an intermediate VH state.

scale in the running coupling α_S; for simplicity, we will set this scale equal to the factorization scale μ throughout.

To explore the μ dependence of the QCD-corrected cross section, we set $\mu = nM_{VH}$, and plot in Fig. 1 both the lowest-order and the QCD-corrected cross sections for $pp \to W^{\pm}H + X$ versus n at the LHC/SSC, for $m_H = 100$ GeV.[2] Also shown are the separate contributions of the $gq \to W^*q$ subprocess and the real and virtual gluon corrections to the $q\bar{q} \to W^*$ subprocess. Set B1 of the Morfin-Tung (MT) distribution functions[14] ($\Lambda = 194$ MeV) in the DIS factorization scheme have been employed. Although the lowest-order cross section is rather sensitive to n, the QCD-corrected cross section is much less so, varying by 5/13 percent throughout the range $1/4 < n < 4$ at the LHC/SSC. We will consider this variation to be an estimate of the theoretical uncertainty in the cross section due to higher orders.

Figure 1 clearly demonstrates that the size of the correction relative to the lowest-order cross section depends on the choice of the factorization scale μ. Thus to claim a given QCD correction without specifying the factorization scale is meaningless. For $\mu = M_{VH}$, the correction amounts to a 17/15 percent increase in the cross section at the LHC/SSC. This is much less than the 25-30 percent increase usually associated with the Drell-Yan process. However, that is the increase in the Drell-Yan process at the $Sp\bar{p}S$/Tevatron; the increase at the LHC/SSC is much less, roughly 16/14 percent.[15] The principal reason for the smaller increase at the LHC/SSC is the increased importance of the $gq \to W^*q$ process. This process, which contributes only a (negative) few percent at the $Sp\bar{p}S$/Tevatron, is negative 8/10 percent at the LHC/SSC for $\mu = M_{VH}$, as a result of the increased luminosity of gluons at smaller

[2] We have used $G_F = 1.166 \times 10^{-5}$ GeV^{-2}, $M_W = 80.14$ GeV, $M_Z = 91.17$ GeV, $sin^2\theta_W^{\overline{MS}} = .2323, cos^2\theta_C = .95, m_t = 140$ GeV, and interpreted the QCD scale given with the parton distribution functions as $\Lambda_4^{\overline{MS}}$ (two loop), and employed the two-loop renormalization-group equation for α_S.

x. The emergence of the $gq \to W^*q$ process at the LHC/SSC invalidates the use of the "approximate K factor", $K = 1 + \frac{\alpha_s}{2\pi}\frac{16}{9}\pi^2$, associated with the soft regions of the real and virtual gluon corrections to the $q\bar{q} \to W^*$ subprocess.

In Fig. 2 we show the same set of curves, but using MT set B1 in the $\overline{\rm MS}$ factorization scheme. The QCD-corrected cross section is nearly invariant under the change in the factorization scheme, as expected. However, the size of the QCD correction relative to the lowest-order cross section is not. For $\mu = M_{VH}$, the QCD correction is positive 12/10 percent at the LHC/SSC. Again, the use of the soft-gluon approximate K factor, which in the $\overline{\rm MS}$ scheme is $K = 1 + \frac{\alpha_s}{2\pi}\frac{8}{9}\pi^2$, is invalidated by the large (negative) contribution of the $gq \to W^*q$ subprocess.

To investigate the dependence of the cross section on the parton distribution functions, we present in Tables 1 and 2 the leading-order (LO) and next-to-leading order (NLO) total cross sections, with $\mu = M_{VH}$, for WH and ZH production at the LHC/SSC for a variety of next-to-leading-logarithm parton distribution functions and Higgs-boson masses. The KMRS[16] sets ($\Lambda = 190$ MeV) are in the $\overline{\rm MS}$ scheme, while the DFLM[17] sets (Λ indicated) are in the DIS scheme, and MT provide sets in both factorization schemes. The size of the correction relative to the lowest-order cross section depends only weakly on the parton distribution functions and the Higgs-boson mass. The KMRS(B_0) and DFLM(360) sets yield the smallest and largest QCD-corrected cross sections, respectively; the ratio is about 1.22/1.43 at the LHC/SSC for $m_H = 100$ GeV, and decreases with increasing Higgs-boson mass. Since the DFLM sets do not contain the recent high-statistics BCDMS data, perhaps this is not a true measure of the uncertainty in the parton distribution functions. Both KMRS and MT contain this data; of these sets, KMRS(B_0) and (B_-) yield the smallest and largest cross sections, respectively, with a ratio of about 1.07/1.20 at the LHC/SSC for $m_H =$

100 GeV. The uncertainty in the cross section due to the parton distribution functions is therefore larger than the uncertainty due to higher orders.

We summarize our numerical results in Fig. 3 by presenting the total cross section for both WH and ZH production versus the Higgs-boson mass at the LHC/SSC, using three different parton distribution functions which span the range of values we have obtained.

Recently, the complete $\mathcal{O}(\alpha_S^2)$ correction to the Drell-Yan process has been completed.[15] It will be worthwhile to include this correction as well once the uncertainty in the parton distribution functions is reduced.

The subprocess $gg \to ZH$, which proceeds via virtual quark loops, also contributes to ZH production at the LHC/SSC.[18] Although formally $\mathcal{O}(\alpha_S^2)$, it is enhanced by the large gluon luminosity. Furthermore, it is independent of other $\mathcal{O}(\alpha_S^2)$ corrections in the sense that it vanishes for a degenerate quark doublet.[3] For $m_H = 100$ GeV and $m_t = 140$ GeV, this subprocess contributes about 5/10 percent of the lowest-order cross section at the LHC/SSC. For $m_H = 140$ GeV and $m_t = 200$ GeV, this contribution is increased to about 25/50 percent. Thus the $gg \to ZH$ subprocess may be as large, or even larger, than the $\mathcal{O}(\alpha_S)$ correction which we have calculated. There is no analogous process for WH production, of course.

Since detectors are generally limited in their coverage, the question arises as to how sensitive our results are to cuts on the final-state particles. Since we have integrated over the final-state phase space, we cannot address this issue. However, we can restrict the rapidity of the parton CM frame with respect to the lab frame. Although this is not experimentally accessible, it gives us some idea of the effect of making cuts on

[3] There are $\mathcal{O}(\alpha_S^2)$ corrections to the Drell-Yan process which also vanish for a degenerate quark doublet, but they are very small.[19]

the rapidities of the final-state particles. We found that our qualitative results are insensitive to making this restriction, indicating that they are applicable even when rapidity cuts are made on the final-state particles. We are presently calculating the QCD-corrected differential cross section to address this issue directly.

To summarize, we have found that if we set the factorization scale equal to the invariant mass of the VH final state, the QCD correction to the total cross section for $pp \to VH + X$ is about positive 17/15 percent in the DIS scheme, and 12/10 percent in the $\overline{\rm MS}$ scheme, at the LHC/SSC. The QCD-corrected cross section is insensitive to the choice of the factorization scale. The largest remaining uncertainty is due to the parton distribution functions.

Acknowledgements:

We are grateful for conversations with S. Keller and W.-K. Tung regarding parton distribution functions. S. W. thanks Fermilab for its hospitality while this work was being completed.

References

[1] R. Johnson, presented at the SSC Physics Symposium, University of Wisconsin, Madison, Feb. 25-27, 1991.

[2] T. Rizzo, Phys. Rev. D**22** (1980) 722; W.-Y. Keung and W. Marciano, Phys. Rev. D**30** (1984) 248.

[3] J. Gunion, G. Kane, and J. Wudka, Nucl. Phys. **B299** (1988) 231.

[4] J. Ellis, M. K. Gaillard, and D. V. Nanopoulos, Nucl. Phys. **B106** (1976) 292; J. Leveille, Phys. Lett. **83B** (1979) 123; A. Vainshtein, M. Voloshin, V. Zakharov, and M. Shifman, Yad. Fis. **30** (1979) 1368 [Sov. J. Nucl. Phys. **30** (1979) 711].

[5] S. Glashow, D. V. Nanopoulos, and A. Yildiz, Phys. Rev. D**18** (1978) 1724.

[6] R. Kleiss, Z. Kunszt, and W. J. Stirling, Phys. Lett. **253B** (1991) 269.

[7] M. Mangano, SDC Collaboration Note SSC-SDC-90-00113.

[8] Z. Kunszt, Nucl. Phys. **B247** (1984) 339; J. Gunion, H. Haber, F. Paige, W.-K. Tung, and S. Willenbrock, Nucl. Phys. **B294** (1987) 621; D. Dicus and S. Willenbrock, Phys. Rev. D**39** (1989) 751.

[9] W. Marciano and F. Paige, BNL–45805 (1991).

[10] J. Gunion, UCD-91-2 (1991).

[11] J. Gunion and G. Kane, UCD-91-0010, to appear in *Proceedings of the 1990 DPF Summer Study on High Energy Physics: Research Directions for the Decade*, Snowmass, CO, 1990.

[12] G. Altarelli, R. K. Ellis, and G. Martinelli, Nucl. Phys. **B157** (1979) 461; J. Kubar-André and F. Paige, Phys. Rev. D**19** (1979) 221.

[13] For a pedegogical treatment, see S. Willenbrock in *From Actions to Answers, Proceedings of the 1989 Theoretical Advanced Study Institute (TASI)*, eds. T. DeGrand and D. Toussaint (World Scientific, Singapore, 1990), p. 323.

[14] J. Morfin and W.-K. Tung, FERMILAB-PUB-90/74, to appear in Z. Phys.

[15] R. Hamberg, W. van Neerven, and T. Matsuura, DESY-90-129 (1990).

[16] J. Kwiecinski, A. Martin, R. Roberts, and W. J. Stirling, Phys. Rev. D**42** (1990) 3645.

[17] M. Diemoz, F. Ferroni, E. Longo, and G. Martinelli, Z. Phys. **C39** (1988) 21.

[18] D. Dicus and C. Kao, Phys. Rev. D**38**(1988) 1008; B. Kniehl, Phys. Rev. D**42** (1990) 2253.

[19] D. Dicus and S. Willenbrock, Phys. Rev. D**34** (1986) 148.

Table Captions

Table 1: Total cross sections (pb) for $pp \to W^{\pm}H + X$ (sum of $W^{+}H$ and $W^{-}H$) at the (a) LHC and (b) SSC, at leading order (LO) and next-to-leading order (NLO) in QCD, for several Higgs-boson masses (GeV). The factorization scale has been set equal to the WH invariant mass.

Table 2: Total cross sections (pb) for $pp \to ZH + X$ at the (a) LHC and (b) SSC, at leading order (LO) and next-to-leading order (NLO) in QCD, for several Higgs-boson masses (GeV). The factorization scale has been set equal to the ZH invariant mass.

Table 1 (a)

WH	LHC	MT		KMRS		DFLM		
m_H		B1-DIS	B1-$\overline{\text{MS}}$	B_0	B_-	160	260	360
80	LO	4.40	4.39	4.22	4.50	4.09	4.53	4.87
	NLO	5.14	4.90	4.67	5.05	4.76	5.36	5.85
100	LO	2.39	2.38	2.29	2.43	2.24	2.44	2.59
	NLO	2.80	2.66	2.56	2.74	2.62	2.90	3.12
120	LO	1.41	1.40	1.36	1.42	1.33	1.43	1.50
	NLO	1.65	1.57	1.52	1.60	1.55	1.70	1.80
140	LO	0.88	0.87	0.85	0.89	0.83	0.89	0.92
	NLO	1.03	0.98	0.96	1.00	0.96	1.05	1.10

Table 1 (b)

WH	SSC	MT		KMRS		DFLM		
m_H		B1-DIS	B1-$\overline{\text{MS}}$	B_0	B_-	160	260	360
80	LO	11.3	11.2	10.6	12.8	10.0	12.2	14.4
	NLO	13.1	12.4	11.5	14.1	11.4	14.2	16.9
100	LO	6.33	6.28	5.96	6.99	5.68	6.82	7.89
	NLO	7.31	6.92	6.47	7.74	6.47	7.90	9.22
120	LO	3.83	3.79	3.58	4.13	3.44	4.07	4.65
	NLO	4.42	4.18	3.94	4.59	3.95	4.75	5.49
140	LO	2.45	2.42	2.30	2.60	2.21	2.58	2.91
	NLO	2.83	2.66	2.52	2.89	2.52	3.02	3.44

Table 2 (a)

ZH	LHC	MT		KMRS		DFLM		
m_H		B1-DIS	B1-$\overline{\text{MS}}$	B_0	B_-	160	260	360
80	LO	2.38	2.40	2.24	2.35	2.22	2.44	2.60
	NLO	2.76	2.65	2.47	2.64	2.55	2.86	3.10
100	LO	1.33	1.33	1.25	1.31	1.24	1.34	1.41
	NLO	1.54	1.46	1.38	1.46	1.42	1.57	1.68
120	LO	0.79	0.79	0.75	0.78	0.74	0.79	0.83
	NLO	0.92	0.87	0.83	0.87	0.85	0.93	0.98
140	LO	0.50	0.50	0.48	0.49	0.47	0.50	0.51
	NLO	0.58	0.55	0.53	0.54	0.54	0.58	0.61

Table 2 (b)

ZH	SSC	MT		KMRS		DFLM		
m_H		B1-DIS	B1-$\overline{\text{MS}}$	B_0	B_-	160	260	360
80	LO	6.35	6.34	5.77	6.84	5.65	6.85	8.01
	NLO	7.27	6.91	6.24	7.52	6.37	7.86	9.32
100	LO	3.62	3.61	3.29	3.82	3.23	3.86	4.44
	NLO	4.14	3.92	3.57	4.20	3.66	4.44	5.19
120	LO	2.22	2.20	2.02	2.30	1.99	2.34	2.66
	NLO	2.53	2.40	2.19	2.53	2.26	2.69	3.11
140	LO	1.43	1.42	1.31	1.46	1.29	1.50	1.68
	NLO	1.63	1.54	1.42	1.61	1.47	1.73	1.97

Figure Captions

Fig. 1: The total cross section for $pp \to W^{\pm}H + X$ (sum of $W^{+}H$ and $W^{-}H$) at the (a) LHC and (b) SSC, for $m_H = 100$ GeV, as a function of the factorization-scale parameter n, where $\mu = nM_{WH}$. The lowest-order cross section, QCD-corrected cross section, and the separate contributions of the $gq \to W^{*}q$ subprocess (gq order α_S) and the real and virtual gluon corrections to the $q\bar{q} \to W^{*}$ subprocess ($q\bar{q}$ order α_S) are shown. Set B1 of the Morfin–Tung parton distribution functions in the DIS scheme has been used.

Fig. 2: Same as Fig. 1, but in the $\overline{\text{MS}}$ scheme.

Fig. 3: The QCD-corrected total cross sections for $pp \to W^{\pm}H + X$ (sum of $W^{+}H$ and $W^{-}H$) and $pp \to ZH + X$ at the (a) LHC and (b) SSC versus the Higgs-boson mass for three different sets of parton distribution functions.

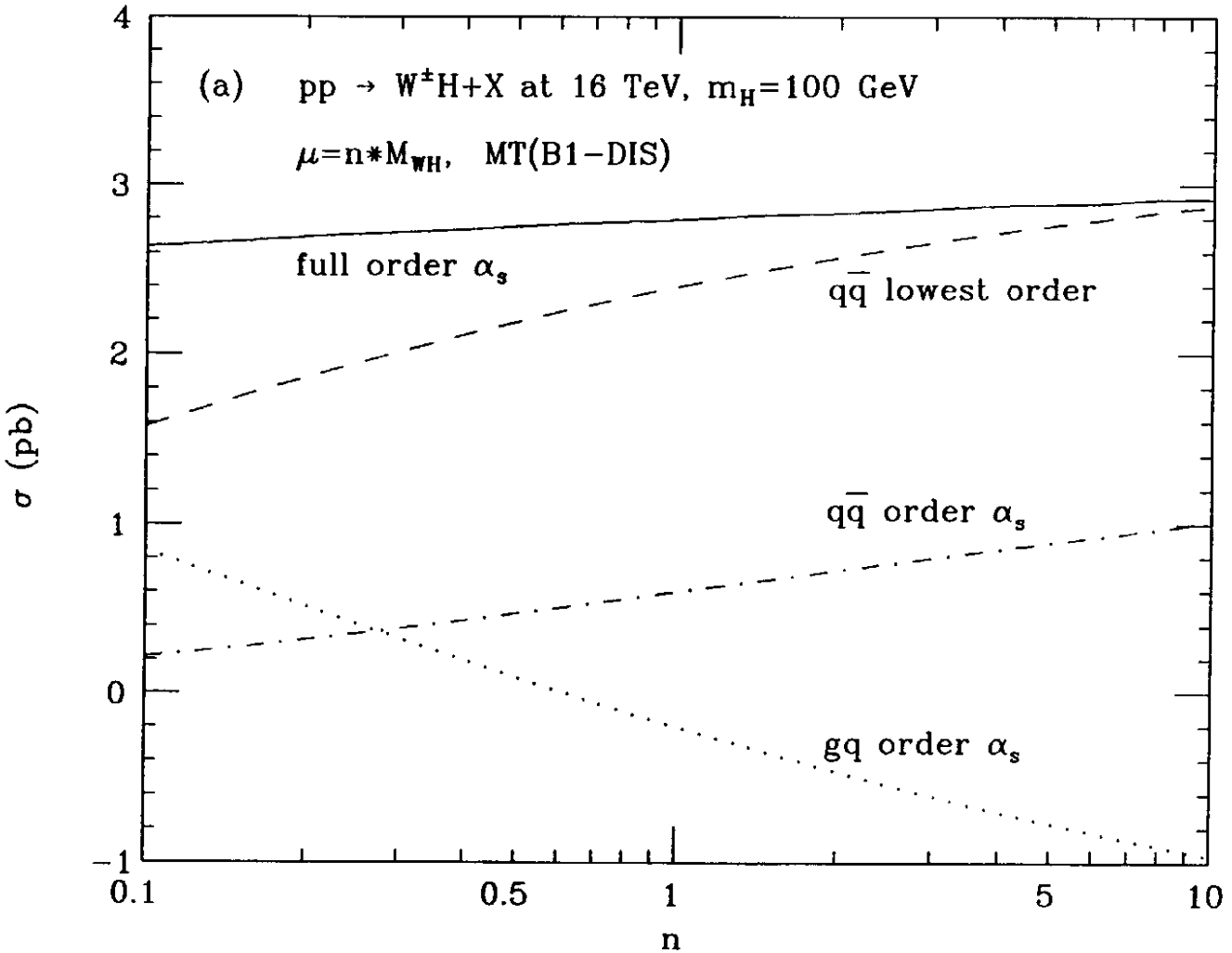
(a) pp → W±H+X at 16 TeV, m_H=100 GeV
μ=n*M_WH, MT(B1-DIS)
full order α_s
qq̄ lowest order
qq̄ order α_s
gq order α_s
σ (pb)
n
4
3
2
1
0
−1
0.1
0.5
1
5
10

Fig. 1(a)

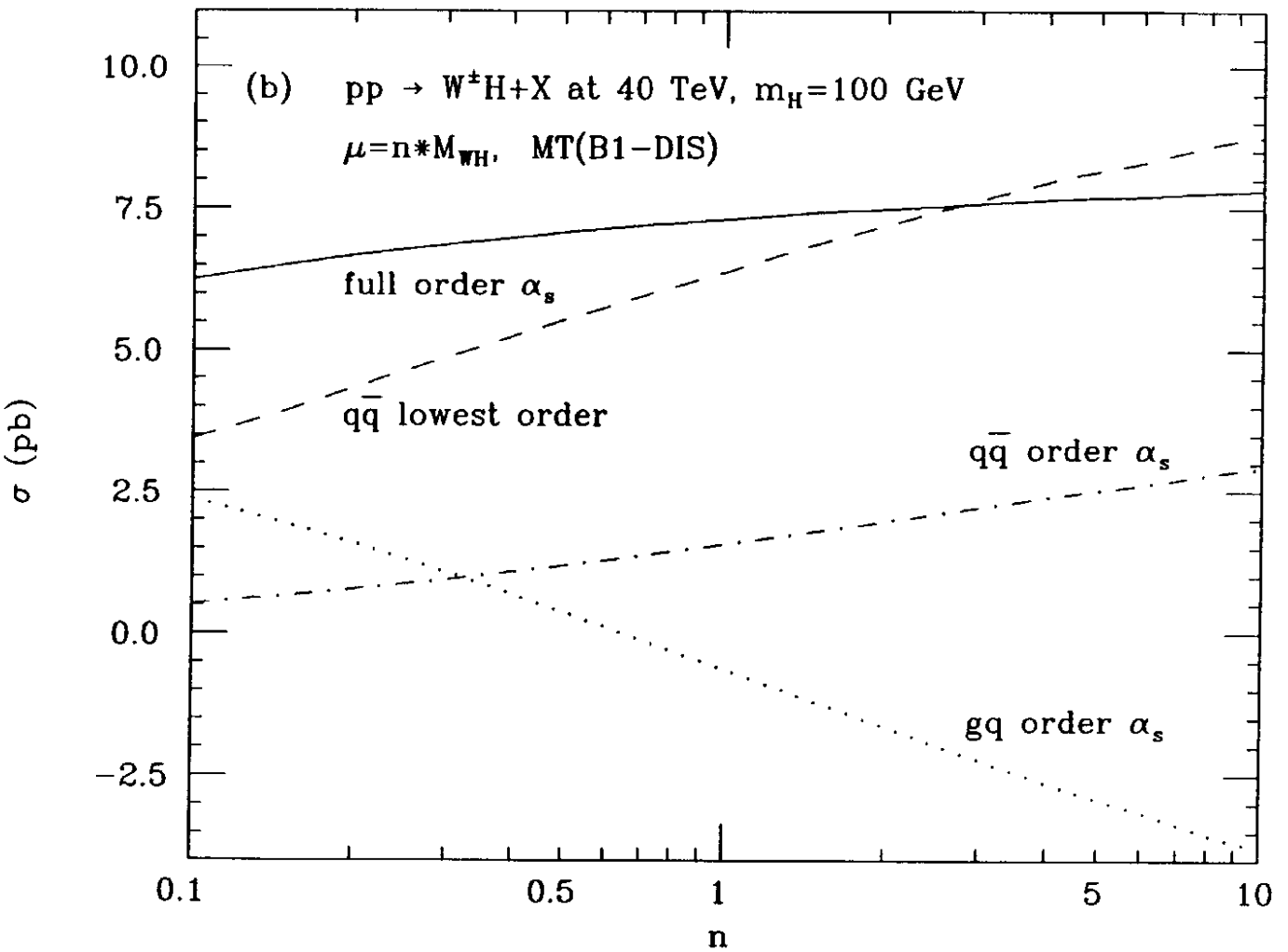
(b) pp → W±H+X at 40 TeV, m_H=100 GeV
μ=n*M_WH, MT(B1-DIS)
full order α_s
qq̄ lowest order
qq̄ order α_s
gq order α_s
σ (pb)
n
10.0
7.5
5.0
2.5
0.0
-2.5
0.1
0.5
1
5
10

Fig. 1(b)

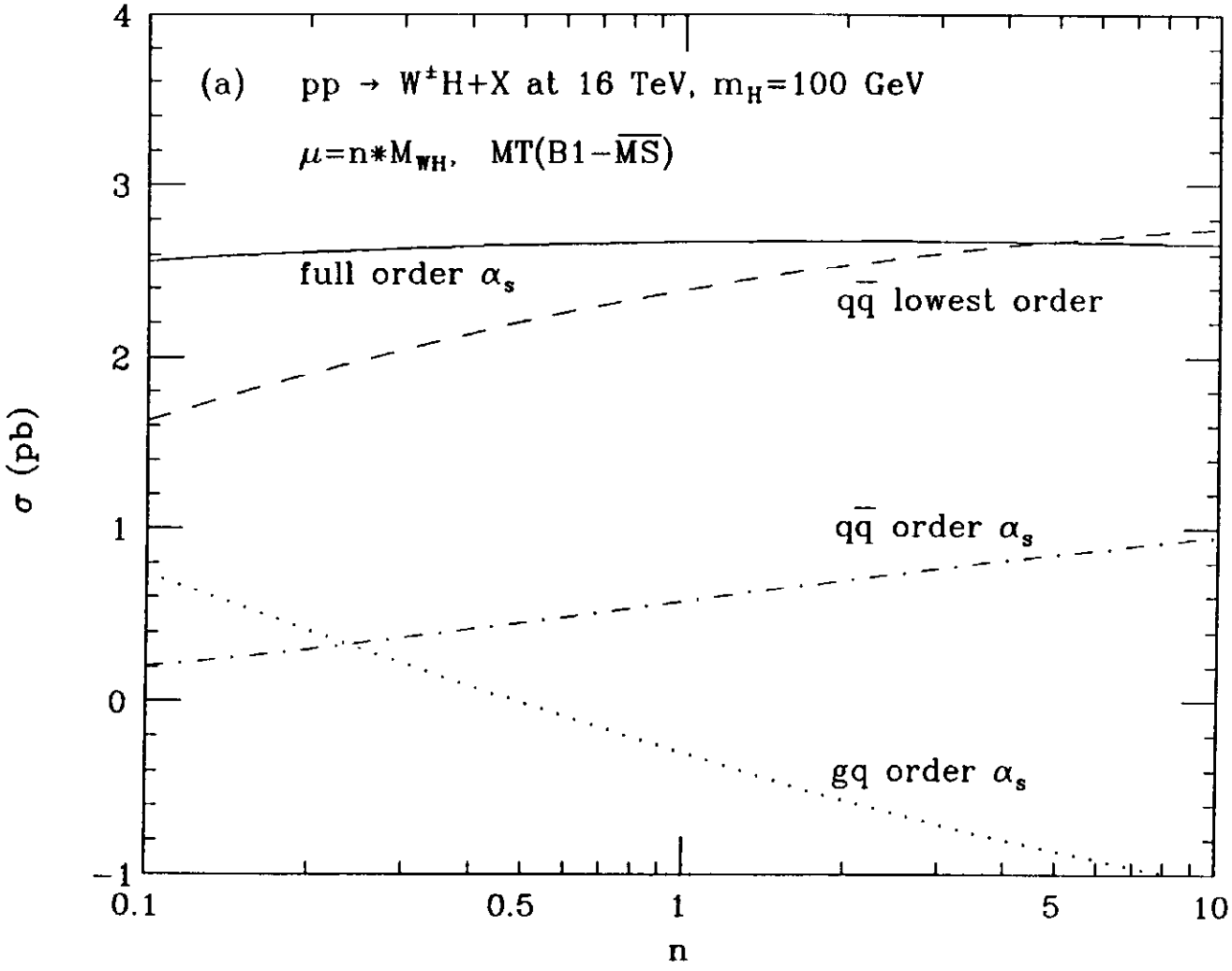
(a) pp → W±H+X at 16 TeV, m_H=100 GeV
μ=n*M_WH, MT(B1−MS̄)
full order α_s
qq̄ lowest order
qq̄ order α_s
gq order α_s
σ (pb)
n
4
3
2
1
0
−1
0.1
0.5
1
5
10

Fig. 2(a)

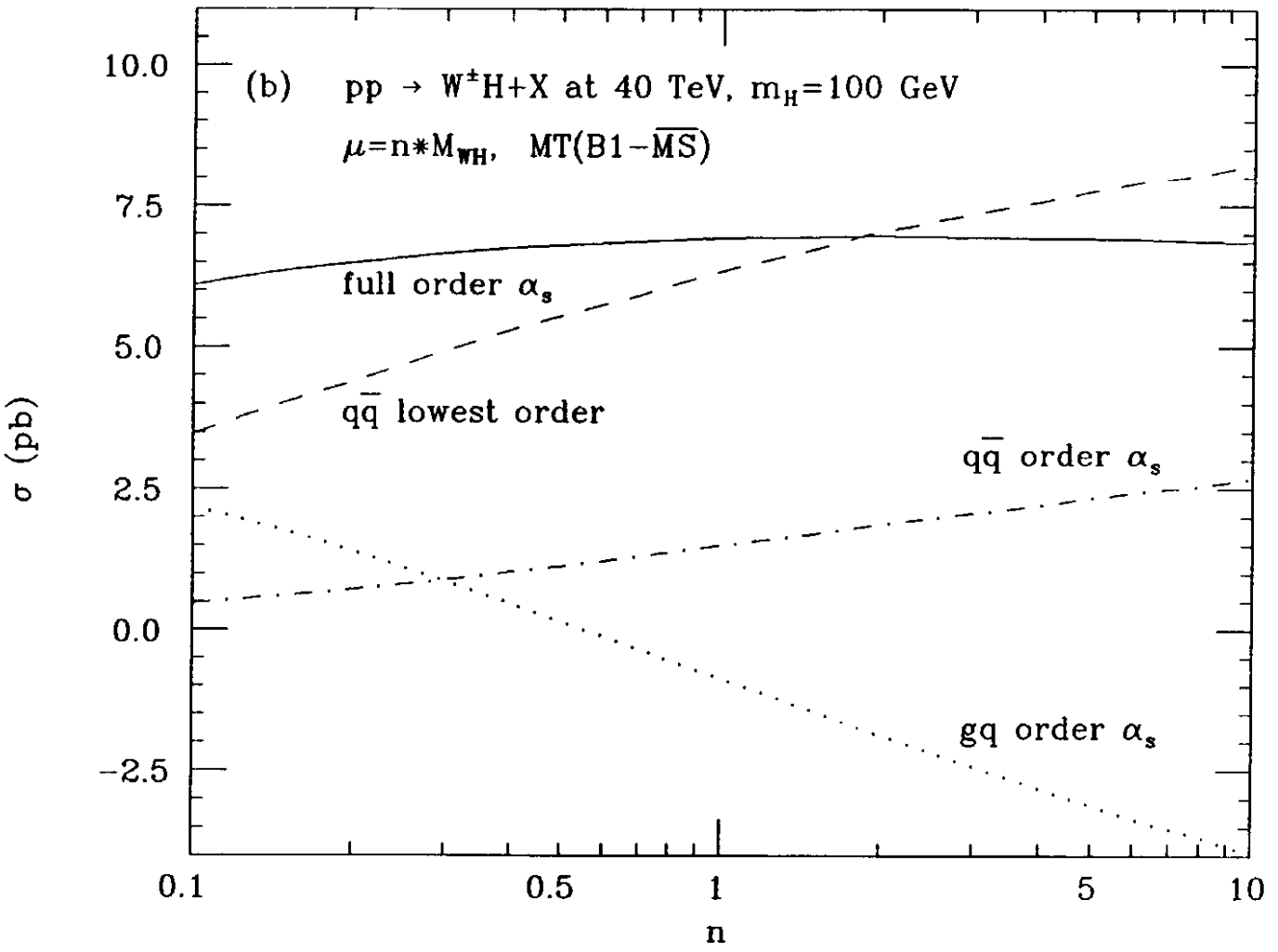
(b) pp → W±H+X at 40 TeV, m_H=100 GeV
μ=n*M_WH, MT(B1−MS)
full order α_s
qq̄ lowest order
qq̄ order α_s
gq order α_s
σ (pb)
n
10.0
7.5
5.0
2.5
0.0
−2.5
0.1
0.5
1
5
10

Fig. 2(b)

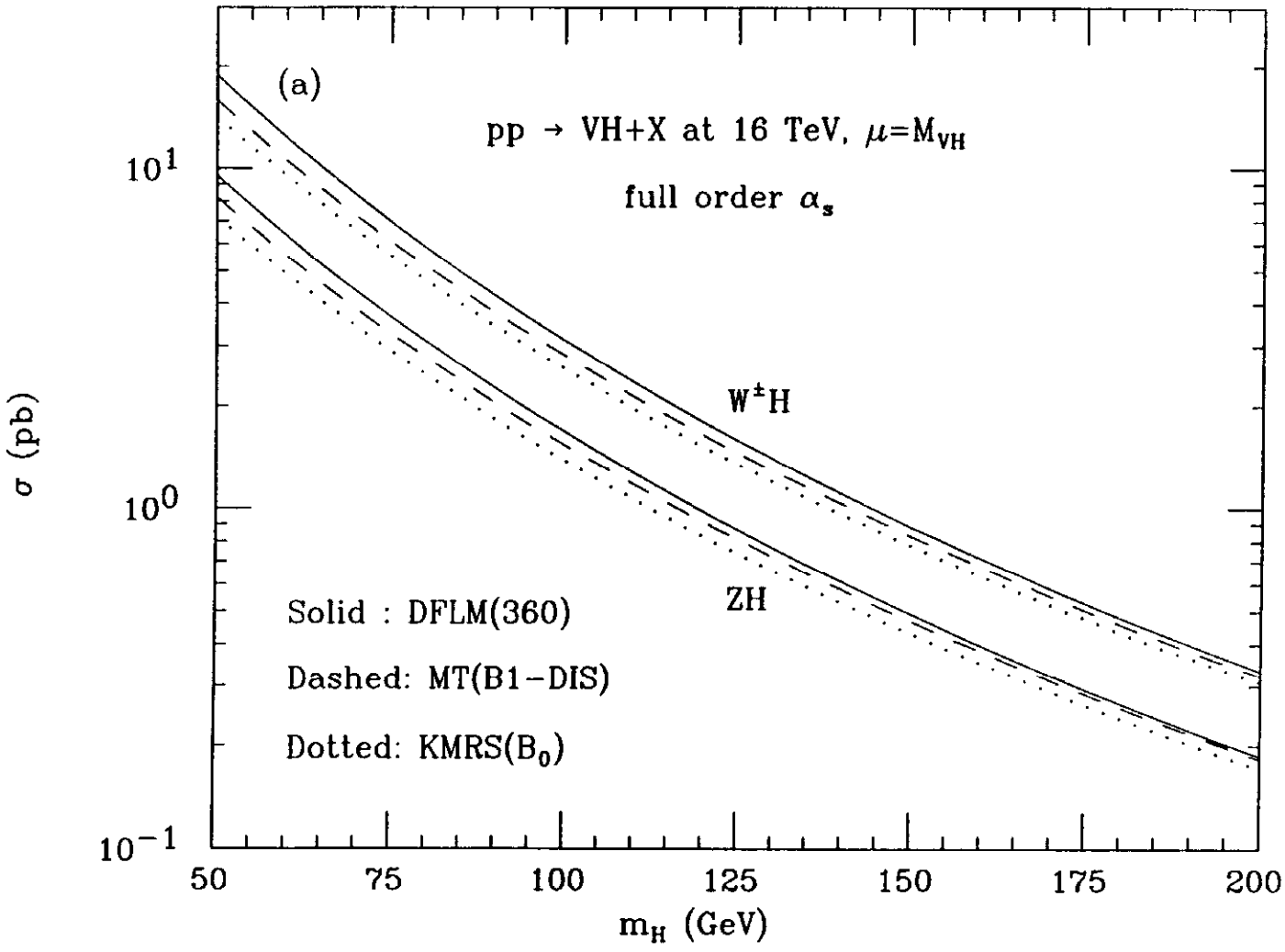
(a)
pp → VH+X at 16 TeV, μ=M_VH
full order α_s
W±H
ZH
Solid : DFLM(360)
Dashed: MT(B1-DIS)
Dotted: KMRS(B0)
σ (pb)
10^1
10^0
10^-1
50
75
100
125
150
175
200
m_H (GeV)

Fig. 3(a)

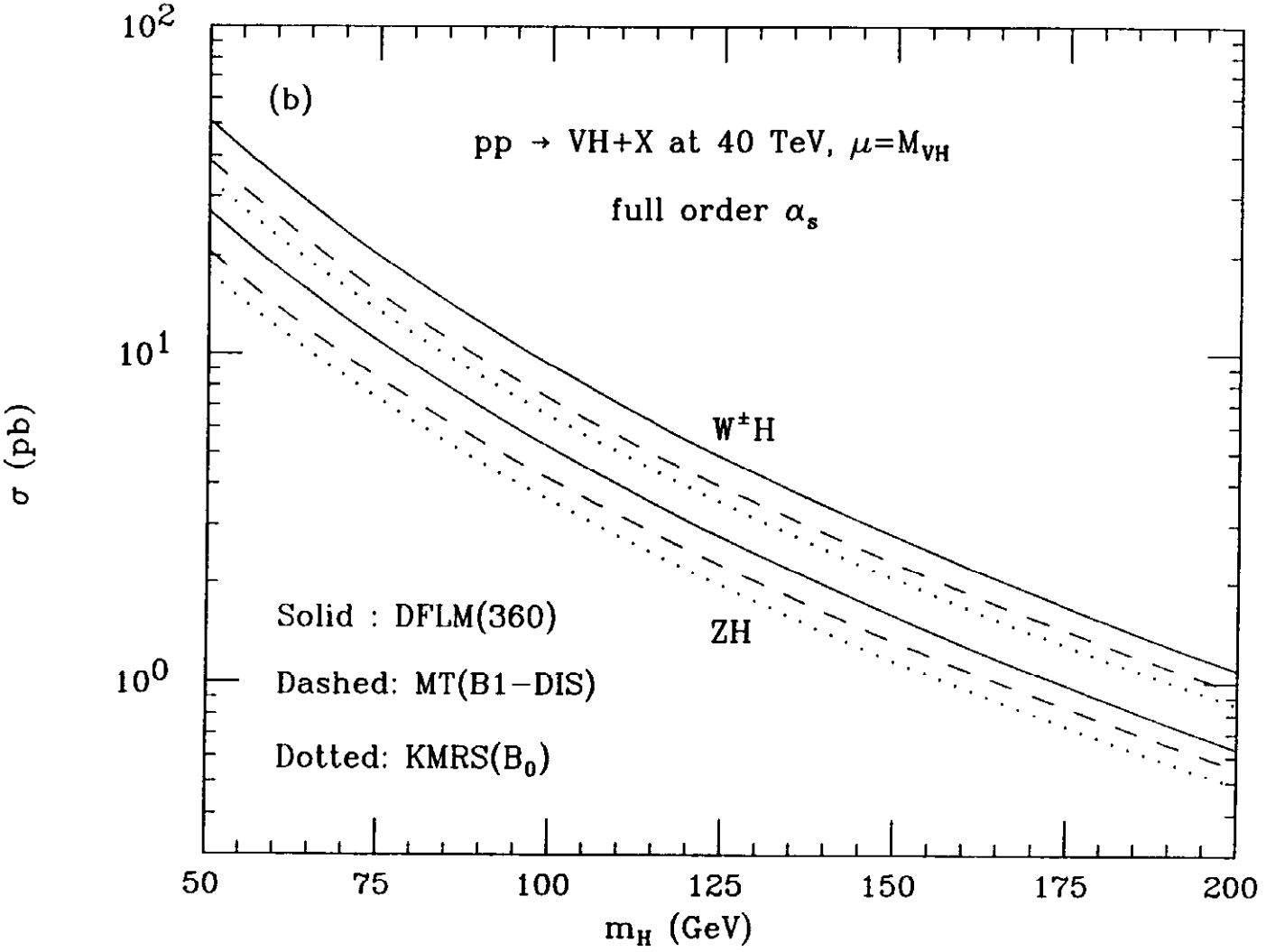
(b)
pp → VH+X at 40 TeV, μ=M_VH
full order α_s
W±H
ZH
Solid : DFLM(360)
Dashed: MT(B1−DIS)
Dotted: KMRS(B_0)
σ (pb)
10^2
10^1
10^0
50
75
100
125
150
175
200
m_H (GeV)

Fig. 3(b)